Ali KHAQAN[1], Sardar Muhammad GULFAM[1], Laeeq RIAZ[1], Azhar YASIN[1], Abrar AHMED[1], Mohsin JAMIL[3], Bakhtiar ALI[1], , Haider ALI[1], Fahad SHARIEF[1], Raja Ali RIAZ[1,2]

Department of Electrical Engineering, COMSATS Institute of Information Technology, Islamabad (1), School of ECS, University of Southampton (2), National University of Science and Technology, Islamabad (3)

Performance of Time Hopping Impulse Radio in Ultrawideband Propagation Channels: Implications of UWB and Diversity Order Selection

Abstract. *In this treatise, we quantify the effects of the UltraWideBand (UWB) on Time Hopping (TH) Impulse Radio (IR) operating in UWB propagation channels environment in terms of bandwidth utilization through diversity order selection. We select L strongest MultiPath Components (MPC) from N_r resolvable MPCs using Maximal Ratio Combining (MRC) in order to achieve maximum performance gain in single and full load scenarios. Three classical detectors have being used for analysis purposes named Correlation (Corr), Zero Forcing Detector (ZFD) and Minimum Mean Square Error (MMSE). Our results suggest that the diversity order L of 20 achieves maximum gain of 18dB and 12dB in single and full load N_u of 63 users scenarios, having spreading factor N_s of 63 over no diversity configuration. Hence, MPCs with delays greater than the TH chip time T_c are resolved by synchronization with the initial path of the received signal gives maximum performance gain.*

Streszczenie. *W artykule przedstawiono wyniki analizy dotyczącej działania techniki Time Hopping Impulse Radio, zastosowanej w komunikacji Ultra WideBand, pod kątem stopnia wykorzystania dostępnej przepustowości. W analizie zastosowano trzy typy detektorów: Corr, ZFD, MMSE. Wyniki badań wskazują, że gdy komponenty wielościeżkowe o opóźnieniach większych niż okres Time Hopping są synchronizowane z początkiem odbieranego sygnału, osiągana jest maksymalna efektywność działania.* ***(Działanie techniki Time Hopping Impulse Radio w komunikacji Ultra Wide-Band – zastosowanie UWB oraz doboru stopnia różnorodności)****.*

Keywords: UWB, Diversity Order, Time Hopping, Impulse Radio
Słowa kluczowe: UWB, stopień różnorodności, Time Hopping, Impulse Radio.

Introduction

UltraWideBand (UWB) radio communicates with baseband pulses of very short duration, typically on the order of a nanosecond, thereby spreading the energy of the radio signal very thinly (about a few μW per MHz) from near DC to a few Gigahertz. Because of the very broad spectrum of this signal, which we typically associate with an impulse function, this is also called Impulse radio. The most popular implementation is not a carrier-based system. It is a baseband system having a Power Spectral Density (PSD) that occupies frequencies from near DC to a few Gigahertz. UWB technology is based on sending and receiving very high bandwidth carrierless radio impulses using extremely accurate timing [1].

One benefit of UWB systems is that with a sufficiently wide transmission bandwidth (BW), it is possible to resolve the closely spaced multipath components (MPC) encountered in the channel. Unlike systems using narrowband transmissions assume most of the closely spaced multipath components as a single faded signal. Hence, by proper synchronization with the initial path of the received signal, large number of multipath components can be resolved for high probability detection.

Maximal ratio combining represents a theoretically optimal combiner over fading channels as a diversity scheme in a communication system. Theoretically, multiple copies of the same information signal are combined so as to maximise the instantaneous SNR at the output. Complexity and performance issues have motivated studies of multipath combining receivers that process only a subset of the available resolved multipath components, However, the number of MPCs that can be utilized are limited by power consumption issues, design complexity, and the channel estimation [2].

A comprehensive statistical model is described in [3] for UWB propagation channels that is valid for a frequency range from 3 to 10 GHz. It was accepted by the IEEE 802.15.4a Task Group as standard model for evaluation of UWB system proposals. The model includes the frequency dependence of the path gain as well as several generalizations of the Saleh–Valenzuela model [4], like mixed Poisson times of arrival and delay-dependent cluster decay constants.

In this contribution, we have used statistical model of UWB propagation channels [3] for indoor environment parameters to quantify the effects of the UWB-TH-IR in terms of bandwidth utilization through diversity order selection.We select L strongest MPCs from N_r resolvable MPCs using MRC in order to achieve maximum performance gain in single and full load scenarios. The performance analysis is provided for three classical detectors i.e. Correlation (Corr), Zero Forcing Detector (ZFD) and Minimum Mean Square Error (MMSE). The respective gains achieved through diversity order for different detectors are detailed. This concept is an alternative to Mutli-Antenna transmission.

The remaining paper is organised as follows. Firstly the system model is elaborated. The UWB-TH-IR transmission and detectors are explained in next section. Third section represents the simulation results and discussion. Finally, we present our conclusions and future work.

System Model

Fig. 1 is the schematic of the scheme considered in this paper. 16-ary symbols are transmitted within a TH interval T_H with a rate of R_H. We have considered slow TH therefore the ratio of signalling interval duration T_s to TH interval T_H is less than 1. As shown in Fig. 1, during a signalling interval duration of T_s seconds, b message bits of the kth user are loaded into the symbol buffer. We denote the symbol as $\zeta^{(k)}$ where $\zeta^{(k)} \in \{0, 1, \cdots, 16\}$ being 16-ary signalling. The 16-ary symbol $\zeta^{(k)}$ is temporarily stored in the buffer, where it awaits its time-slot, in which it is transmitted. Since a slow TH scheme frame duration T_f is equal to T_s therefore each transmitted time-domain pulse $\Psi(t)$ conveys a 16-ary symbol. In this contribution we have used Orthogonal Prolate Spheroidal Wave Function for signalling pulse $\Psi(t)$ generated by the pulse generator.

As shown in Fig. 1, the transmitter generates a time-domain pulse $\Psi(t - jT_f)$, where j represents the frame index, $\Psi(t)$ is defined within the interval of $[0, T_h)$ and is normalized such that we have $\int_0^{T_h} \Psi^2(t)$=T_h in the context of each 16-ary symbol. In Fig. 1, $\upsilon^{(k)}$ represents the Pesudo-Noise (PN) code based TH pattern assigned to user

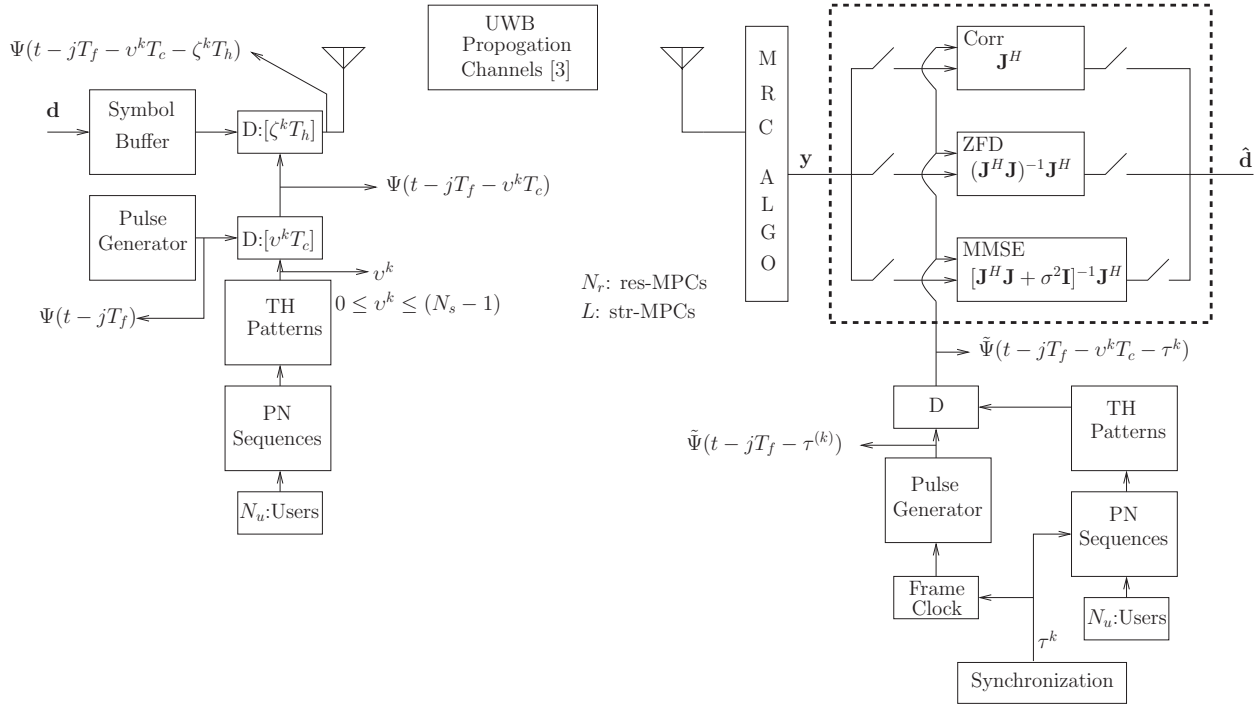

Figure 1. Schematic of UWB-TH-IR system with N_r resolvable MPCs and L strongest MPCs and three detectors in UWB propagation channels.

k, where $\upsilon^{(k)}$ are integers assuming values in the range of $0 < \upsilon^{(k)} \le (N_s - 1)$ where N_s is the spreading factor. The TH pattern imposes a PN-code dependent time shift on the pulse during every frame. Each PN code dependent time shift is a discrete time value given by $\upsilon^{(k)} T_c$ obeying $0 < \upsilon^{(k)} T_c \le (N_s - 1)T_c$. In the context of 16-ary pulse position baseband modulation, one of the 16 possible time slots within the TH chip determined by the TH pattern is activated for transmission, signalling the presence of a pulse. The 16-ary symbol $\zeta^{(k)}$ assuming a value from the range of $0 < \zeta^{(k)} \le 16$ imposes a further $\zeta^{(k)} T_h$ seconds of information symbol dependent time shift on the time domain pulse position $\Psi(t)$, as shown in Fig. 1. Then the combined singal of N_u users is transmitted.

After transmission over a UWB propagation channels [3] based on indoor channel measurements between 3.1 GHZ to 10.6 GHz over a range of less than 10 meters contaminated by Additive White Gaussian Noise (AWGN) having a variance of $\frac{N_o}{2}$ per dimension, the signal is fed into a MRC block, as shown in Fig. 1. MRC combines MPCs so as to maximise the instantaneous SNR at the output. In this paper, we select L strongest MPC from N_r resolvable MPCs. After MRC block, the received singal $\mathbf{y}$ is fed into the detectors block supported by the information required to estimate the received data $\hat{\mathbf{d}}$.

Three detectors Corr, ZFD and MMSE are used to estimate the data $\hat{\mathbf{d}}$ on selection. Based on the knowledge of path delays $\tau^{(k)}$, the pulse generator generates a time domain pulse $\Psi(t - jT_f - \tau^{(k)})$ for the jth frame and the TH pattern generator outputs the corresponding TH pattern value or synonymously, the address code $\upsilon^{(k)}$, as shown in Fig. 1. The TH pattern $\upsilon^{(k)}$ provides a time shift of $\upsilon^{(k)} T_c$ seconds for the time-domain pulse $\Psi(t - jT_f - \tau^{(k)})$, which yields $\Psi(t - jT_f - \upsilon^{(k)} T_c - \tau^{(k)})$. This information is provided to each detector to estimate the data $\hat{\mathbf{d}}$. In the next section we briefly explain the UWB transmission and detection schemes.

UWB Transmission and Detection

Transmitted Signal

A general UWB-TH-IR signal is given by [1]

$$s^{(k)}(t) = \sum_{j=-\infty}^{\infty} \Psi(t - jT_f - \upsilon_j^{(k)} T_c - \zeta_j^{(k)} T_h), \quad (1)$$

where $\Psi(t)$ is reference pulse shape, T_f is the frame time, $\upsilon_j^{(k)}$ represents the PN code based TH pattern assigned to user k, T_c is the time shift based on TH code where the code repeats after a certain interval, $\zeta_j^{(k)}$ corresponds to user k data symbols, T_h is small shift in the pulse position, either forward or backward to represent the data symbol. The pulse repetition frequency (PRF) is reciprocal of T_F. The frame time T_F will be of the order of 1000 times the actual pulse width to avoid interference from reflected pulses.

Channel Model

In this contribution, UWB-TH-IR is evaluated using UWB multipath channel model based on indoor channel measurements between 3.1 GHZ to 10.6 GHz over a range of 7 to 10 meters [3]. Here we detail few mandatory equations of the channel model which are used in our analysis. The impulse response (in complex baseband) of the Saleh-Valenzuela (SV) model is given in general as [4]

$$h(t) = \sum_{l=0}^{L} \sum_{k=0}^{K} \alpha_{(k,l)} e^{(\psi_{(k,l)})} \delta(t - T_l - \tau_{k,l}) \quad (2)$$

where $\alpha_{(k,l)}$ is the tap weight of the kth component in the lth cluster, T_l is the delay of the lth cluster, and $\tau_{k,l}$ is the delay of the kth MPC relative to the lth cluster arrival time T_l. The phases $\psi_{(k,l)}$ are uniformly distributed, i.e., for a bandpass system, the phase is taken as a uniformly distributed random variable from the range $[0, 2\pi]$. The number of clusters L is modeled as Poisson-distributed with probability density func-

tion (PDF)

$$pdf_L(L) = \frac{(\overline{L})^L e^{-\overline{L}}}{L!} \tag{3}$$

so that the mean $\overline{L}$ completely characterizes the distribution.

By definition, we have $\tau_{(0,l)} = 0$. The distributions of the cluster arrival times are given by a Poisson process so that the inter-cluster arrival times are exponentially distributed

$$p(T_l/T_{l-1}) = \Lambda_l e^{[-\Lambda_l(T_l - T_{l-1})]}, l > 0 \tag{4}$$

where Λ_l is the cluster arrival rate (assumed to be independent of l). The ray arrival times is a mixture of two Poisson processes as follows [5]:

$$p(\tau_k/\tau_{k-1,l}) = \beta\lambda_1 e^{[-\lambda_1(\tau_{k,l} - \tau_{k-1,l})]} + (1-\beta)\lambda_2 \tag{5}$$

where β is the mixture probability, while λ_1 and λ_2 are the ray arrival rates. The mean power of the different paths is exponential within each cluster

$$E\{\mid \alpha_{(k,l)} \mid^2\} \propto \Omega_l e^{(\frac{-\tau_{k,l}}{\gamma_l})} \tag{6}$$

where Ω_l is the integrated energy of the lth cluster and γ_l is the intracluster decay time constant. The energy of the lth cluster, normalized to γ_l and averaged over the cluster shadowing and the small-scale fading, follows in general an exponential decay

$$10log(\Omega_l) \propto 10log\big(e^{(\frac{-T_l}{\Gamma})}\big) + M_{cluster} \tag{7}$$

where $M_{cluster}$ is a normally distributed variable with standard deviation $\sigma_{cluster}$ and Γ is cluster power-decay time constant.

Detection Schemes

The discretized received composite signal can be represented in matrix form as [6]:

$$\mathbf{y} = \mathbf{Jd} + \mathbf{n}, \tag{8}$$

where $\mathbf{n}$ is the noise sequence consisting of noise samples that are zero mean Gaussian variables having a variance of σ^2 and has a covariance matrix of $\mathbf{R}_n = E[nn^H]$, $\mathbf{J}$ is overall system matrix and $\mathbf{d}$ is users data vector.

Corr Detector: The correlation detector is constituted by two filtering stages. The pre-whitening filter [6] is followed by the matched filter. The data estimates at the output of detector is

$$\hat{\mathbf{d}}_{\mathbf{Corr}} = \underbrace{diag(\mathbf{J^H R_n^{-1} J})\mathbf{d}}_{Data} + \underbrace{\overline{diag}(\mathbf{J^H R_n^{-1} J})\mathbf{d}}_{ISI,MAI} + \underbrace{\mathbf{J^H R_n^{-1} n}}_{noise}, \tag{9}$$

The composite form for data estimates from Eq (9) with I as an identity matrix is given by

$$\hat{\mathbf{d}}_{\mathbf{Corr}}\Big|_{\mathbf{R}_n=\sigma^2 I} = \mathbf{J^H y}, \tag{10}$$

The Corr detector simply estimates the data and fails to balance Multi-Access Interference (MAI) and Inter-Symbol Interference (ISI) produced by the multiuser and multipath environment.

ZFD Detector: The ZFD is similar to the zero-forcing linear equalizer [6]. The data estimates at the output of ZFD is

$$\hat{\mathbf{d}}_{\mathbf{ZFD}} = \underbrace{\mathbf{d}}_{Data} + \underbrace{(\mathbf{J^H R_n^{-1} J})^{-1}\mathbf{J^H R_n^{-1} n}}_{Noise}, \tag{11}$$

Eq (11) with I as identity matrix can be reduced to

$$\hat{\mathbf{d}}_{\mathbf{ZFD}}\Big|_{\mathbf{R}_n=\sigma^2 I} = (\mathbf{J^H J})^{-1}\mathbf{J^H y}, \tag{12}$$

It is evident from Eqs (11) and (12) that ZFD decorrelates the MAI and ISI and forces them to zero. However the removal of ISI and MAI is performed at the expense of noise enhancement.

MMSE Detector: The MMSE detector minimises the simple quadratic form [7]

$$Q(\hat{\mathbf{d}}) = E\left[(\mathbf{d} - \hat{\mathbf{d}})^H(\mathbf{d} - \hat{\mathbf{d}})\right], \tag{13}$$

where $\hat{\mathbf{d}}$ is the estimate of the data $\mathbf{d}$. The MMSE detector's estimated bits $\hat{\mathbf{d}}_{MMSE}$ can be expressed as

$$\begin{aligned}\hat{\mathbf{m}}_{MMSE} &= \underbrace{diag\Big(\big[\mathbf{I} + (\mathbf{R}_d\mathbf{J}^H\mathbf{R}_n^{-1}\mathbf{J})^{-1}\big]^{-1}\Big)\mathbf{d}}_{Data} \\ &+ \underbrace{\overline{diag}\Big(\big[\mathbf{I} + (\mathbf{R}_d\mathbf{J}^H\mathbf{R}_n^{-1}\mathbf{J})^{-1}\big]^{-1}\Big)\mathbf{d}}_{ISI,MAI} \\ &+ \underbrace{(\mathbf{J}^H\mathbf{R}_n^{-1}\mathbf{J} + \mathbf{R}_d^{-1})^{-1}\mathbf{J}^H\mathbf{R}_n^{-1}\mathbf{n}}_{noise}.\end{aligned} \tag{14}$$

where R_d is the covariance matrix of the data symbols, I is the identity matrix. Eq (14) can be reduced to

$$\hat{\mathbf{d}}_{\mathbf{MMSE}}\Big|_{\mathbf{R}_n=\sigma^2 I, \mathbf{R}_d=I} = [\mathbf{J^H J} + \sigma^{\mathbf{2}}\mathbf{I}]^{-\mathbf{1}}\mathbf{J^H y}, \tag{15}$$

From Equations (14) and (15), it can be seen that the MMSE detector attempts to achieve a balance between eliminating the different types of data impairments including the noise, MAI and ISI in order to minimize the mean squared estimation error in the simple quadratic form given in Eq (13).

Simulation Results and Discussion

In order to simulate the real scenario, we have used UWB propagation channels model based on indoor channel measurements between 3.1 GHZ to 10.6 GHz over a range of 7 to 10 meters [3]. We have considered the corner cases of single user $N_u = 1$ and full load $N_u = 63$ scenarios. The spreading factor $N_s = 63$ is being employed. The selection of diversity order L from N_r resolvable MPCs is being done by MRC algorithm. The L strongest MPCs have the 85% of the energy from N_r resolvable paths. Table 1 illustrates the channel parameters values discussed in Section III and used in our simulations.

The data burst length per user N is a parameter which simulates the effects of ISI. Therefore $N = 1000$ and $N_u = 63$ in our simulations gives high level of ISI and MAI, which has to be mitigated through diversity order. The diversity order $L = 20$ from $N_r = 30$ resolvable MPCs has the same effect of transmitting through multiple antennas. However, the number of MPCs that can be utilized are limited by power consumption issues, design complexity, and the channel estimation. Table 2 illustrates the simulation system parameters being used in our simulation. Fig. 2 gives the overview of the detection state flow.

Table 1. PARAMETERS FOR CHANNEL MODELS CM 1 AND CM 2 (RESIDENTIAL)

Residential	LOS	NLOS
valid Range of d	7-20m	7-20m
$G_0[dB]$	-43.9	-48.7
$\overline{L}$	3	3.5
$\Lambda[1/ns]$	0.047	0.12
$\lambda_1, \lambda_2[1/ns], \beta$	1.54,0.15,0.095	1.77,0.15,0.045
$\Gamma[ns]$	22.61	26.27
k_γ	0	0
$\gamma_0[ns]$	12.53	17.50
$\sigma_{cluster}$	2.75	2.93

Table 2. Simulation System Parameters

Spreading Factor	$0 < N_s \leq 63$
No. of Users	$N_u = 1, 3, 13, 23, 33, 43, 53, 63$
Data Burst Length Per User	$N = 1000$
Number of Resolvable Paths	$N_r = 30$
Number of Strongest Paths	$L = 1, 5, 10, 20$
Detector I	Corr
Detector II	ZFD
Detector III	MMSE

*Assumptions:*We have assumed that the receiver has achieved synchronization for the received signal, the receiver has the perfect knowledge of the transmission delay of τ^k. Furthermore, we assume that the receiver employs a TH pattern replica, which is generated by a local PN generator as shown in Fig. 1.

Fig. 3 shows the performance gain of UWB-TH-IR system in case of single user $N_u = 1$ with diversity order $L = 20$ from $N_r = 30$ resolvable paths. As the Fig. 3 depicts the ZFD and MMSE achieve the performance close to the AWGN with the mentioned diversity order from $L = 1$ no diversity gain scenario. The respective gains of 18dB and 16dB for ZFD and MMSE is portrayed at high $\frac{E_b}{N_o}$ values. There is no improvement in Corr detection as lacking the capability of mitigating ISI.

Fig. 4 shows the performance gain of UWB-TH-IR system in case of full load $N_u = 63$ with diversity order $L = 20$ from $N_r = 30$ resolvable paths and spreading factor $N_s = 63$. As the Fig. 4 depicts the ZFD and MMSE achieve the performance gain with the mentioned diversity order from $L = 1$ no diversity gain scenario. The respective gains of 5dB and 12dB for ZFD and MMSE is portrayed at high $\frac{E_b}{N_o}$ values. The ZFD performs badly at lower $\frac{E_b}{N_o}$ values since it enhances the noise as shown in Eqs (11) and (12). Finally, Fig. 5 depicts the trend of performance gain in case of MMSE detector with varying diversity order L and number of users N_u at $\frac{E_b}{N_o}$=10dB.

Conclusion and future work

We have investigated the performance gain of UWB-TH-IR system with diversity selection operating in UWB propagation channels. Since UWB provides an extra bandwidth for transmission of the information signals therefore diversity through resolvable paths can be utilized for high probability detection, unlike narrowband transmission. However, the number of MPCs that can be utilized are limited by power consumption issues, design complexity, and the channel estimation. More explicitly, we have shown that selecting L number of strongest paths from N_r resolvable paths gives remarkable performance gain, supported by exhaustive simulation parameters. Furthermore, we have detailed the performance gain in extreme MAI and ISI simulation environment

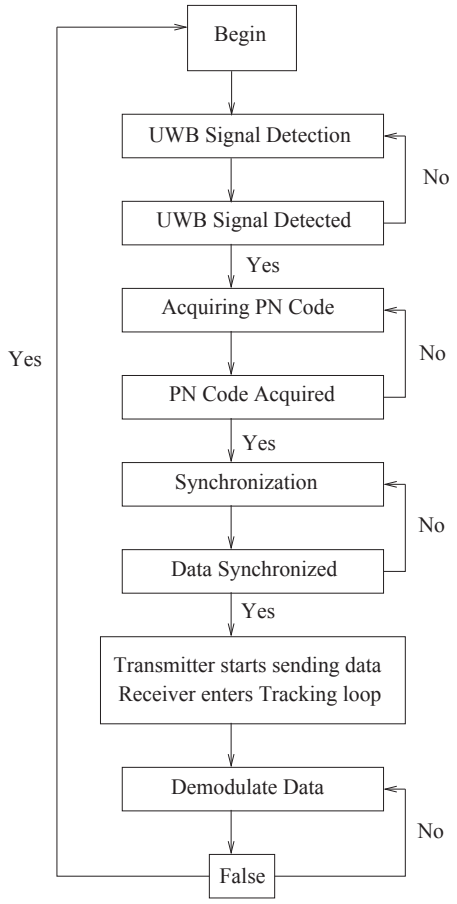

Figure 2. UWB-TH-IR detection state flow diagram.

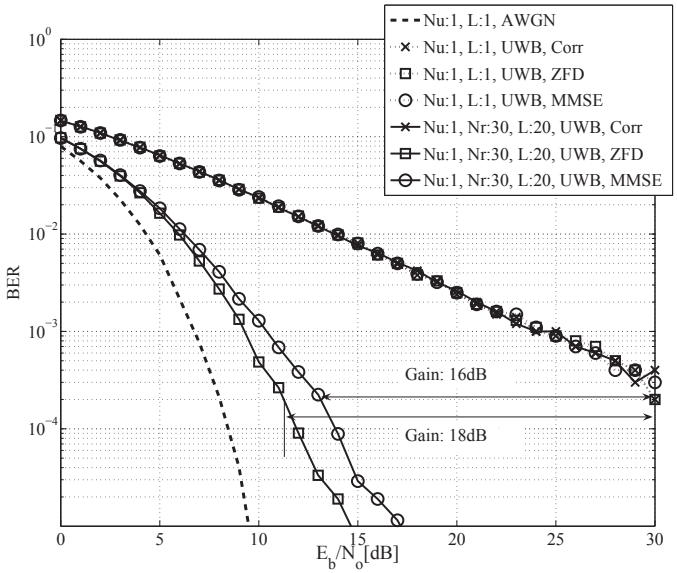

Figure 3. BER vs $\frac{E_b}{N_o}$[dB] for UWB-TH-IR system with users $N_u = 1$, diversity order $L = 20$, resolvable MPCs $N_r = 30$ and spreading factor $N_s = 63$.

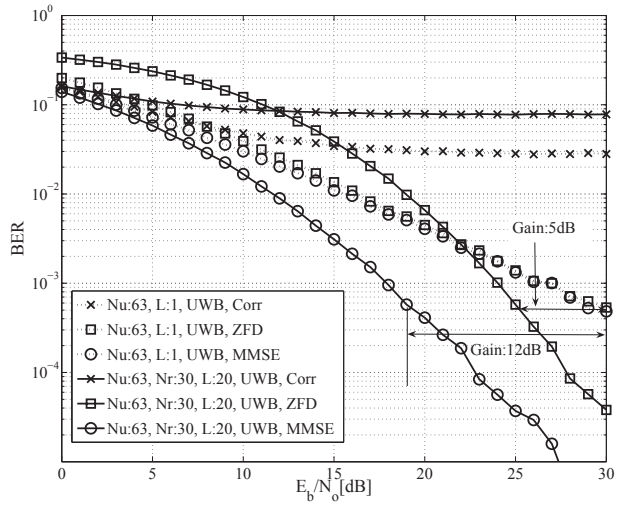

Figure 4. BER vs $\frac{E_b}{N_o}$[dB] for UWB-TH-IR system with users $N_u = 63$, diversity order $L = 20$, resolvable MPCs $N_r = 30$ and spreading factor $N_s = 63$.

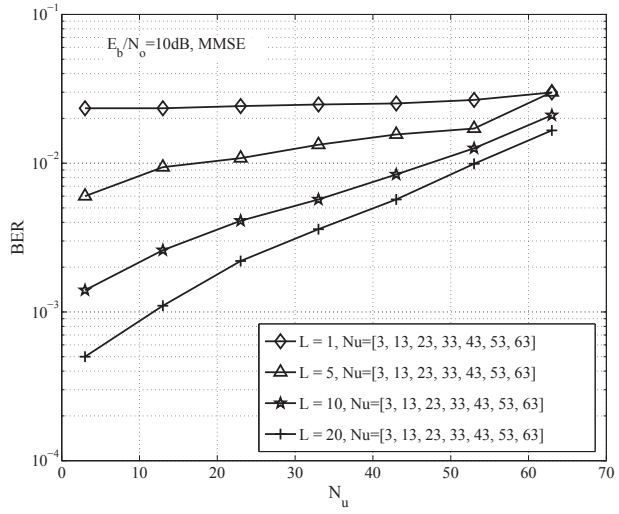

Figure 5. N_u vs BER for UWB-TH-IR with MMSE detector, $\frac{E_b}{N_o}$=10[dB], mentioned diversity order L and nubmer of users N_u, showing the trend of performance gain with diversity order increase.

of three classical detection schemes. If this diversity selection technique is appropriately utilized, this can be answer to multiple antennas.

In our future work, we will investigate more sophisticated iterative decoding scheme, through exchange of extrinsic information amongst the detector, in order to achieve near-capacity performance of UWB-TH-IR system.

Acknowledgements

The authors would like to thank the staff of Multi-Processor Lab at University of Southampton for their support and patience in exhaustive simulations, running for long durations.

REFERENCES

[1] Win, M. Z. and Scholtz, R. A.: Impulse radio: how it works, IEEE Communications Letters, pp. 36–38, 1998.

[2] Win, M. Z. and Scholtz, R. A.: On the energy capture of ultra-wide bandwidth signals in densemultipath environments, IEEE Communications Letters, pp. 245–247, 1998.

[3] Molisch, A. F. and Cassioli, D. and Chong, C. -C. and Emami, S. and Fort, A. and Kannan, B. and Karedal, J. and Kunisch, J. and Schantz, H. G. and Siwiak, K. and Win, M. Z.: A Comprehensive Standardized Model for Ultrawideband Propagation Channels, IEEE Transactions on Antennas and Propagation, pp. 3151–3166, 2006.

[4] Saleh, A. and Valenzuela, R.: A Statistical Model for Indoor Multipath Propagation, IEEE Journal on Selected Areas in Communications, pp. 128–137, 1987.

[5] Chia-Chin Chong and Su Khiong Yong: A Generic Statistical-Based UWB Channel Model for High-Rise Apartments, IEEE Transactions on Antennas and Propagation, pp. 2389–2399, 2005.

[6] L. Hanzo and L-L. Yang and E-L. Kuan and K. Yen: Single- and Multi-Carrier DS-CDMA: Multi-User Detection, Space-Time Spreading, Synchronisation, Networking and Standards, John Wiley and Sons, England, 2003.

[7] Klein, A. and Kaleh, G. K. and Baier, P. W.: Zero forcing and minimum mean-square-error equalization formultiuser detection in code-division multiple-access channels, IEEE Transactions on Vehicular Technology, pp. 276–287, 1996.

***Authors**: Sardar Muhammad Gulfam (MS, Finland)and Abrar Ahmed (MS, UK), Associate Prof. Raja A. Riaz (Ph. D.), Electrical Engineering Department, COMSATS Institute of Information Technology (http://ciitisb.edu.pk), Park Road, Chak Shehzad Campus, 44000, Islamabad, Pakistan, email: rajaali@comsats.edu.pk*